Computing sparse affine-linear control policies for linear power flow in microgrids

Edwin Mora & Florian Steinke
Energy Information Networks and Systems
Technische Universität Darmstadt, Germany
{edwin.mora, florian.steinke}@eins.tu-darmstadt.de

***Abstract*—We determine affine-linear control policies for linear power systems that are robust against variations of nodal power injections. The paper presents a novel way to compute such policies with a minimal number of controller and sensor devices by solving a single mixed-integer linear optimization problem. The developed algorithm is then applied to a demonstrative microgrid with 4 buses as well as to a modified version of the IEEE 30 bus power system. We show that sparse control realizations with minimal configurations of controllers and measurements are obtained efficiently for both systems.**

***Index Terms*—Controllability, observability, optimization, power flow, resilience**

I. Introduction

The integration of distributed energy resources and electric vehicles into the power grid requires new power flow control methods to guarantee feasible grid operation in the presence of increased supply and demand uncertainty. In this context, we aim to control some active power injections such that the feasibility of the resulting power flow is guaranteed for all possible values of the remaining non-controlled injections. The control set points are computed for each situation based on the information provided by a given set of measurement devices. Assuming a linear power flow model and constraining the control policy to be affine-linear, we then ask: What is the minimum number of power injections to be controlled based on the smallest number of measurements so that such a control policy can be found? Obtaining sparse but robust control policies is beneficial for reducing communication and computation efforts of the control system. It thereby saves costs and installation efforts. Moreover, if the minimal set of controllers and measurements is protected especially well, feasible system operation can be guaranteed even if the remaining elements are damaged by natural disasters or compromised by cyber-attacks. The approach would then also help improving power grid operational resilience.

The design of the desired sparse affine-linear control policy can be understood as an instance of the *optimal input/output selection problem*, also known as *optimal actuator/sensor placement problem* [1]. Such kind of optimization problems have recently gained importance in the analysis of stability, controllability, and observability of complex networks. However, current theoretical methods for solving the input/output selection problem are mostly based on the topology of the network only, i.e., they can provide optimal solutions as long as the studied system has no state or input/output restrictions.

On the other hand, several approaches have been proposed for power flow analysis under interval uncertainties during the last decade, where most of them are robust power flow formulations based on affine interval arithmetic [2]–[5]. In addition, an approach for optimal robust power flow with a linear power flow model is presented in [6]. Besides generator set points, they also compute the primary control parameters of a given set of generators to achieve feasible grid operation when the injections of other set of producers and consumers are uncertain. The minimization of the required controller/sensor sets is not considered in any of these works.

This contribution incorporates the optimal selection of actuators and sensors into robust power flow control. It extends the idea proposed recently in [7], where a greedy hill climbing approach is used to find the minimal possible set of controllers and sensors for an affine-linear control policy. In this paper, we show that the design of such a policy can also be posed as a mixed-integer linear program (MILP). This leads to a more efficient approach. Moreover, the MILP can be solved to global optimality or stopped early with provable sub-optimality guarantees.

The rest of the paper is structured as follows: The linear power flow model utilized for our numerical experiments is presented in Section II. A formal problem statement is then given in Section III. In Section IV, we develop a mixed-integer linear program that minimizes the number of controllers and sensors required to implement the affine-linear control policy. In Section V, we apply the proposed algorithm to 1) a simple microgrid consisting of 4 buses connected in line topology and 2) a modified version of the IEEE 30 bus test case. Concluding remarks and an outlook for future research are provided in Section VI.

II. Linear Power Flow

We analyze an electrical network with N electrical buses connected by T transmission lines under the common *DC power flow* assumptions [8]. The voltage phase angles $\boldsymbol{\theta} \in \mathbb{R}^N$

This work was sponsored by the German Federal Ministry of Education and Research in project AlgoRes (grant no. 01jS18066A). It has been performed in the context of the LOEWE center emergenCITY.

determine the nodal active power injections $\boldsymbol{p}_{\mathrm{I}} \in \mathbb{R}^N$ and the active power line flows $\boldsymbol{p}_{\mathrm{F}} \in \mathbb{R}^T$ as

$$\boldsymbol{p}_{\mathrm{I}} = \mathbf{B}_{\mathrm{I}}\boldsymbol{\theta}, \quad \boldsymbol{p}_{\mathrm{F}} = \mathbf{B}_{\mathrm{F}}\boldsymbol{\theta}, \tag{1}$$

where the entries of $\mathbf{B}_{\mathrm{I}} \in \mathbb{R}^{N\times N}$ and $\mathbf{B}_{\mathrm{F}} \in \mathbb{R}^{T\times N}$ are defined element-wise as $B_{\mathrm{I},jk} = -b_{jk}$ if $j \neq k$, $B_{\mathrm{I},jj} = \sum_k b_{jk}$ and $B_{\mathrm{F},jk} = b_{jk}$, with b_{jk} the susceptance of the line connecting buses j and k.

Without loss of generality, we assume that exactly one generator or load is connected to each bus, with an externally defined active power set point x_i. If the sum of the set points in the grid is not balanced, a *droop-based primary control* scheme [8] adjusts power injections $\boldsymbol{p}_{\mathrm{I}}$ under adaptation of the frequency to achieve this balance,

$$\boldsymbol{p}_{\mathrm{I}} = \boldsymbol{x} - \boldsymbol{k}\Delta\omega. \tag{2}$$

Here, $\boldsymbol{k} \in \mathbb{R}^N$ represents the vector of droop constants, $k_i \geq 0$ and $\sum_i k_i > 0$, and $\Delta\omega \in \mathbb{R}$ the frequency deviation with respect to its nominal value.

This common setup implies that the measurable quantities $\boldsymbol{p}_{\mathrm{I}}$, $\boldsymbol{p}_{\mathrm{F}}$, and $\Delta\omega$ are linearly determined by the controllable quantities $\boldsymbol{x}$. The kernel of the Laplacian matrix $\mathbf{B}_{\mathrm{I}}$ contains only the constant vectors for connected graphs, that is, a constant shift of the phase angles has no impact on $\boldsymbol{p}_{\mathrm{I}}$. We thus fix $\theta_1 = 0$ and delete the first column of $\mathbf{B}_{\mathrm{I}}$ to obtain $\tilde{\mathbf{B}}_{\mathrm{I}}$. The remaining dimensions of $\boldsymbol{\theta}$ are denoted by $\tilde{\boldsymbol{\theta}}$. We similarly reduce $\mathbf{B}_{\mathrm{F}}$ to $\tilde{\mathbf{B}}_{\mathrm{F}}$. The image of $\tilde{\mathbf{B}}_{\mathrm{I}}$ moreover contains all vectors with balanced nodal injections. To handle unbalanced set points $\boldsymbol{x}$, we add $\boldsymbol{k}$ as the last column. This lets us compute for all $\boldsymbol{x}$ with $\cdot$ denoting zero entries

$$\begin{bmatrix} \boldsymbol{p}_{\mathrm{I}} \\ \boldsymbol{p}_{\mathrm{F}} \\ \Delta\omega \end{bmatrix} = \begin{bmatrix} \tilde{\mathbf{B}}_{\mathrm{I}} & \cdot \\ \tilde{\mathbf{B}}_{\mathrm{F}} & \cdot \\ \cdot & 1 \end{bmatrix} \begin{bmatrix} \tilde{\boldsymbol{\theta}} \\ \Delta\omega \end{bmatrix} = \begin{bmatrix} \tilde{\mathbf{B}}_{\mathrm{I}} & \cdot \\ \tilde{\mathbf{B}}_{\mathrm{F}} & \cdot \\ \cdot & 1 \end{bmatrix} \begin{bmatrix} \tilde{\mathbf{B}}_{\mathrm{I}} & \boldsymbol{k} \end{bmatrix}^{-1} \boldsymbol{x}. \tag{3}$$

In real systems the nodal injections $\boldsymbol{p}_{\mathrm{I}}$ will be limited above and below by the technical capabilities of the connected generator or load. Valid set points $\boldsymbol{x}$ might be restricted to smaller intervals than the $\boldsymbol{p}_{\mathrm{I}}$, to leave some space for power generation scheduled by the primary controller. Similarly, line power flows $\boldsymbol{p}_{\mathrm{F}}$ and the frequency deviation $\Delta\omega$ are typically subject to upper and lower bounds.

III. Problem Statement

We represent the linear power flow presented in the previous section as the following set of linear (in)equalities:

$$\mathbf{A}\boldsymbol{x} \leq \boldsymbol{b}, \tag{4a}$$

$$\boldsymbol{y} = \mathbf{M}\boldsymbol{x}, \tag{4b}$$

$$\underline{\boldsymbol{x}} \leq \boldsymbol{x} \leq \overline{\boldsymbol{x}}, \tag{4c}$$

with state $\boldsymbol{x} \in \mathbb{R}^N$, measurements $\boldsymbol{y} \in \mathbb{R}^L$, and parameters $\mathbf{A} \in \mathbb{R}^{K\times N}$, $\boldsymbol{b} \in \mathbb{R}^K$, and $\mathbf{M} \in \mathbb{R}^{L\times N}$. The vector $\boldsymbol{x}$ entirely determines the state of the system and is subject to lower and upper bounds $\underline{\boldsymbol{x}}$ and $\overline{\boldsymbol{x}}$. We partition $\boldsymbol{x}$ into the *controlled* variables $\boldsymbol{x}_{\mathrm{c}}$, for which we will design a control policy in the following, and the *free* variables $\boldsymbol{x}_{\mathrm{f}}$ that are left free to be determined either by other users, cooperative or malicious, by fixed external conditions such as, e.g., the weather, or at random. The index set of the controlled variables is denoted by $\mathcal{C}$.

In Eq. (4b) it is assumed that a set of possible measurements $\boldsymbol{y}$ is related linearly to the system state, with matrix $\mathbf{M}$ being presupposed to have full column rank. The set of measurements $\boldsymbol{y}$ can be partitioned into the *measured* variables $\boldsymbol{y}^{\mathrm{m}}$, which are used as inputs to the control policy, and the *unmonitored* variables $\boldsymbol{y}^{\mathrm{u}}$, which are not required by the control center and may or may be not recorded in practice. The index set of the monitored variables is denoted by $\mathcal{M}$ The defined partitions of $\boldsymbol{x}$ and $\boldsymbol{y}$ allow also to partition matrices $\mathbf{A}$ and $\mathbf{M}$ along their columns and rows, yielding the equivalent representation

$$\mathbf{A}_{\mathrm{c}}\boldsymbol{x}_{\mathrm{c}} + \mathbf{A}_{\mathrm{f}}\boldsymbol{x}_{\mathrm{f}} \leq \boldsymbol{b}, \tag{5a}$$

$$\boldsymbol{y}^{\mathrm{m}} = \mathbf{M}^{\mathrm{m}}\boldsymbol{x}, \tag{5b}$$

$$\begin{bmatrix} \underline{\boldsymbol{x}}_{\mathrm{c}} \\ \underline{\boldsymbol{x}}_{\mathrm{f}} \end{bmatrix} \leq \begin{bmatrix} \boldsymbol{x}_{\mathrm{c}} \\ \boldsymbol{x}_{\mathrm{f}} \end{bmatrix} \leq \begin{bmatrix} \overline{\boldsymbol{x}}_{\mathrm{c}} \\ \overline{\boldsymbol{x}}_{\mathrm{f}} \end{bmatrix}. \tag{5c}$$

In this work, we address the design of an affine-linear control policy

$$\boldsymbol{x}_{\mathrm{c}}(\boldsymbol{y}^{\mathrm{m}}) = \mathbf{S}\boldsymbol{y}^{\mathrm{m}} + \boldsymbol{w}, \tag{6}$$

with static parameters $\mathbf{S} \in \mathbb{R}^{|\mathcal{C}|\times|\mathcal{M}|}$ and $\boldsymbol{w} \in \mathbb{R}^{|\mathcal{C}|}$. $|\mathcal{C}|$ denotes the number of controlled variables and $|\mathcal{M}|$ the number of measured quantities. Note that we consider only controls for the steady-state of the system. We do not examine whether and how it is possible to get there from arbitrary initial positions. The desired policy has to compute the value of the controlled variables based on the information provided by $\boldsymbol{y}^{\mathrm{m}}$ and has to guarantee that the set of linear inequality constraints (4a) are fulfilled for all possible realizations of the free variables $\boldsymbol{x}_{\mathrm{f}}$. This motivates the following definition:

Definition 1: A control policy parametrized by $\mathbf{S}$ and $\boldsymbol{w}$ is admissible if

$$\begin{aligned} \exists \mathbf{S}, \boldsymbol{w} : \forall \boldsymbol{x}_{\mathrm{f}} \in [\underline{\boldsymbol{x}}_{\mathrm{f}}, \overline{\boldsymbol{x}}_{\mathrm{f}}] : \boldsymbol{x}_{\mathrm{c}}(\boldsymbol{y}^{\mathrm{m}}) \in [\underline{\boldsymbol{x}}_{\mathrm{c}}, \overline{\boldsymbol{x}}_{\mathrm{c}}] \wedge \\ \mathbf{A}_{\mathrm{c}}\boldsymbol{x}_{\mathrm{c}}(\boldsymbol{y}^{\mathrm{m}}) + \mathbf{A}_{\mathrm{f}}\boldsymbol{x}_{\mathrm{f}} \leq \boldsymbol{b} \wedge \\ \boldsymbol{x}_{\mathrm{c}}(\boldsymbol{y}^{\mathrm{m}}) = \mathbf{S}\boldsymbol{y}^{\mathrm{m}} + \boldsymbol{w}, \end{aligned} \tag{7}$$

with $\boldsymbol{y}^{\mathrm{m}} = \mathbf{M}^{\mathrm{m}}\boldsymbol{x}$.

Subsequently, we want the admissible control policy to be sparse, i.e., the smallest possible number of entries of $\boldsymbol{x}$ should be manipulated based on the information provided by the smallest possible number of measurements. This is equivalent to finding the minimum possible realization of sets $\mathcal{C}$ and $\mathcal{M}$ that yields an admissible control policy. The sparsest realization of (6) is then the solution of the following optimization task:

$$\begin{aligned} &\min_{\mathcal{C},\mathcal{M}} \; |\mathcal{C}| + \gamma|\mathcal{M}| \\ &\text{s.t.} \;\; \mathcal{C} \text{ and } \mathcal{M} \text{ allow for an admissible control policy.} \end{aligned} \tag{8}$$

The cost of placing a sensor is weighted by $0 \leq \gamma \leq 1$ since it will typically be smaller than implementing a full actuator. Notice that one could alternatively weight the cost of placing each control and sensor device separately. While we do not follow this idea below, the algorithm presented in next section can be straightforwardly be adapted.

IV. Algorithm

In this section we develop a MILP for addressing optimization task (8). The key idea behind the algorithm is to split the problem into two parts: We first describe conditions for an admissible control policy $\hat{\mathbf{S}} \in \mathbb{R}^{N\times L}$, $\hat{\boldsymbol{w}} \in \mathbb{R}^{N}$ that could be used if all nodes are controlled and all measurements are available. We then contrast this with the control policy $\tilde{\mathbf{S}} \in \mathbb{R}^{N\times L}$ that yields the identity $\boldsymbol{x} = \tilde{\mathbf{S}}\mathbf{M}\boldsymbol{x}$, which implies that all variables are free. Since we assume $\mathbf{M}$ to have full column rank, i.e., the state can be reconstructed from all measurements, the second policy $\tilde{\mathbf{S}}$ can be pre-computed as the pseudo-inverse of $\mathbf{M}$. We then use this policy to constrain the structure of $\hat{\mathbf{S}}$ in terms of binary decision variables that encode the selection of controller and measurement devices. The actually applied $\mathbf{S}$ is finally determined by the partition of the resulting $\hat{\mathbf{S}}$ that corresponds to the obtained set of controllers and measurements.

A. Admissibility

According to Definition 1, control policy $\hat{\mathbf{S}}$, $\hat{\boldsymbol{w}}$ must fulfill

$$\underbrace{\begin{bmatrix}\mathbf{A}\hat{\mathbf{S}}\mathbf{M}\\ \hat{\mathbf{S}}\mathbf{M}\\ -\hat{\mathbf{S}}\mathbf{M}\end{bmatrix}}_{\hat{\mathbf{A}}(\hat{\mathbf{S}})}\boldsymbol{x} + \underbrace{\begin{bmatrix}\mathbf{A}\\ \mathbf{I}\\ -\mathbf{I}\end{bmatrix}}_{\hat{\mathbf{A}}_{\mathrm{w}}}\hat{\boldsymbol{w}} \le \underbrace{\begin{bmatrix}\boldsymbol{b}\\ \overline{\boldsymbol{x}}\\ -\underline{\boldsymbol{x}}\end{bmatrix}}_{\hat{\boldsymbol{b}}}, \tag{9}$$

in order to be admissible. Looking at the above inequalities there is an important aspect to highlight: The value of $\hat{\mathbf{S}}$ is determined by the maximum effect of any realization of $\boldsymbol{x}$ on each constraint. For a fixed $\hat{\mathbf{S}}$, the maximum effect of $\boldsymbol{x}$ on inequality (9) can be computed element-wise by using the lower and upper bounds of $\boldsymbol{x}$ in the following manner:

$$H_{ij} = \begin{cases}\hat{A}_{ij}(\hat{\mathbf{S}})\overline{x}_j & \hat{A}_{ij} \ge 0,\\ \hat{A}_{ij}(\hat{\mathbf{S}})\underline{x}_j & \text{else}\end{cases}, \quad \forall i \in \mathcal{I}, \quad \forall j \in \mathcal{J}, \tag{10}$$

with the index sets $\mathcal{I} = \{1, ..., K+2N\}$ and $\mathcal{J} = \{1, ..., N\}$. Thus, the upper bound of $\hat{\mathbf{A}}(\hat{\mathbf{S}})\boldsymbol{x}$ is given by $\mathbf{H}\mathbf{1}$, where $\mathbf{1}$ is a vector of ones with appropriate dimension. Note that the above piecewise expression can also be formulated as a set of linear inequality constraints. To do this, the entries of $\mathbf{H}$ must fulfill

$$\begin{aligned} H_{ij} &\ge \hat{A}_{ij}(\hat{\mathbf{S}})\overline{x}_j, \quad \forall i \in \mathcal{I}, \quad \forall j \in \mathcal{J},\\ H_{ij} &\ge \hat{A}_{ij}(\hat{\mathbf{S}})\underline{x}_j, \quad \forall i \in \mathcal{I}, \quad \forall j \in \mathcal{J}. \end{aligned} \tag{11}$$

B. Structural Constraints

Now consider the binary decision variables $\boldsymbol{u}_{\mathrm{c}} \in \{0,1\}^N$ and $\boldsymbol{u}_{\mathrm{m}} \in \{0,1\}^L$ indicating $\mathcal{C}$ and $\mathcal{M}$, respectively. I.e., the entry x_j is controlled iff $u_{\mathrm{c}j} = 1$ and the variable y_k is measured iff $u_{\mathrm{m}k} = 1$. Moreover, let $\hat{\mathbf{S}}_{\cdot k}$ be the k-th column of $\hat{\mathbf{S}}$, with $k \in \mathcal{K}$ and $\mathcal{K} = \{1, ..., L\}$. In addition, let $\hat{\mathbf{S}}_{j\cdot}$ be the j-row of $\hat{\mathbf{S}}$. We also consider analogous definitions for the rows and columns of $\tilde{\mathbf{S}}$. If a variable x_j is selected as free, then $\hat{\mathbf{S}}_{j\cdot}$ has to match $\tilde{\mathbf{S}}_{j\cdot}$ and $\hat{w}_j$ must be zero. Otherwise, such entries are determined by the optimization algorithm between a pre-defined minimum $\underline{S} \le 0$ and maximum $\overline{S} \ge 0$ value for $\hat{\mathbf{S}}$, and between $\underline{\boldsymbol{x}}$ and $\overline{\boldsymbol{x}}$ for $\hat{\boldsymbol{w}}$. This leads to the linear inequalities

$$\begin{aligned} \underline{S}\,\boldsymbol{u}_{\mathrm{c}} + \tilde{\mathbf{S}}_{\cdot k} \circ (\mathbf{1} - \boldsymbol{u}_{\mathrm{c}}) &\le \hat{\mathbf{S}}_{\cdot k}, \quad \forall k \in \mathcal{K},\\ \hat{\mathbf{S}}_{\cdot k} &\le \overline{S}\,\boldsymbol{u}_{\mathrm{c}} + \tilde{\mathbf{S}}_{\cdot k} \circ (\mathbf{1} - \boldsymbol{u}_{\mathrm{c}}), \quad \forall k \in \mathcal{K}, \end{aligned} \tag{12}$$

and

$$\underline{\boldsymbol{x}} \circ \boldsymbol{u}_{\mathrm{c}} \le \hat{\boldsymbol{w}} \le \overline{\boldsymbol{x}} \circ \boldsymbol{u}_{\mathrm{c}}. \tag{13}$$

Hereby, the operator $\circ$ symbolizes the Hadamard product. Moreover, if variable x_j is controlled and the measurement y_k is not used for its computation, then $\hat{S}_{jk}$ should be zero. This AND condition can be expressed as

$$\begin{aligned} \underline{S}(1 - u_{\mathrm{c}j} + u_{\mathrm{m}k}) &\le \hat{S}_{jk}, \quad \forall j \in \mathcal{J}, \quad \forall k \in \mathcal{K},\\ \hat{S}_{jk} &\le \overline{S}(1 - u_{\mathrm{c}j} + u_{\mathrm{m}k}), \quad \forall j \in \mathcal{J}, \quad \forall k \in \mathcal{K}. \end{aligned} \tag{14}$$

C. Full problem

Putting these results together allows us to find the minimum possible realization of $\boldsymbol{u}_{\mathrm{c}}$ and $\boldsymbol{u}_{\mathrm{m}}$, for which an admissible affine-linear control policy can be computed, via the MILP

$$\begin{aligned} \min_{\substack{\boldsymbol{u}_{\mathrm{c}},\boldsymbol{u}_{\mathrm{m}}\\ \hat{\boldsymbol{w}},\hat{\mathbf{S}},\mathbf{H}}} \quad & \|\boldsymbol{u}_{\mathrm{c}}\|_1 + \gamma\|\boldsymbol{u}_{\mathrm{m}}\|_1\\ \text{s.t}\quad & \mathbf{H}\mathbf{1} + \hat{\mathbf{A}}_{\mathrm{w}}\hat{\boldsymbol{w}} \le \hat{\boldsymbol{b}},\\ & H_{ij} \ge \hat{A}_{ij}(\hat{\mathbf{S}})\overline{x}_j, \quad \forall i \in \mathcal{I}, \quad \forall j \in \mathcal{J},\\ & H_{ij} \ge \hat{A}_{ij}(\hat{\mathbf{S}})\underline{x}_j, \quad \forall i \in \mathcal{I}, \quad \forall j \in \mathcal{J},\\ & \underline{S}(1 - u_{\mathrm{c}j} + u_{\mathrm{m}k}) \le \hat{S}_{jk}, \quad \forall j \in \mathcal{J}, \quad \forall k \in \mathcal{K},\\ & \hat{S}_{jk} \le \overline{S}(1 - u_{\mathrm{c}j} + u_{\mathrm{m}k}), \quad \forall j \in \mathcal{J}, \quad \forall k \in \mathcal{K},\\ & \underline{S}\,\boldsymbol{u}_{\mathrm{c}} + \tilde{\mathbf{S}}_{\cdot k} \circ (\mathbf{1} - \boldsymbol{u}_{\mathrm{c}}) \le \hat{\mathbf{S}}_{\cdot k}, \quad \forall k \in \mathcal{K},\\ & \hat{\mathbf{S}}_{\cdot k} \le \overline{S}\,\boldsymbol{u}_{\mathrm{c}} + \tilde{\mathbf{S}}_{\cdot k} \circ (\mathbf{1} - \boldsymbol{u}_{\mathrm{c}}), \quad \forall k \in \mathcal{K},\\ & \underline{\boldsymbol{x}} \circ \boldsymbol{u}_{\mathrm{c}} \le \hat{\boldsymbol{w}} \le \overline{\boldsymbol{x}} \circ \boldsymbol{u}_{\mathrm{c}}. \end{aligned} \tag{15}$$

The solution of MILP (15) is then used to determine the realization of the parameters $\mathbf{S}$ and $\boldsymbol{w}$ by extracting those partitions that are indicated by $\boldsymbol{u}_{\mathrm{c}}$ and $\boldsymbol{u}_{\mathrm{m}}$ as

$$\boldsymbol{x}_{\mathrm{c}} = \underbrace{\hat{\mathbf{S}}^{\mathrm{c}}_{\mathrm{m}}}_{\mathbf{S}}\,\boldsymbol{y}^{\mathrm{m}} + \underbrace{\hat{\boldsymbol{w}}_{\mathrm{c}}}_{\boldsymbol{w}}. \tag{16}$$

In the next section, we illustrate the applicability of the proposed approach for two exemplary power systems.

V. Numerical Experiments

The algorithm developed in IV is now applied to find the minimal configuration of controllers and measurements required to design the affine-linear control policy for two exemplary power systems. We first demonstrate our setup and typical effects on a simple microgrid of 4 buses connected in a line. Subsequently, a modified version of the IEEE 30 bus test case is addressed. An i5 notebook with 8 GB of RAM was used when performing the MILP optimization for both power systems. We use $\gamma = 0.5$ for solving (15) in all experiments.

A. Simple microgrid

The considered microgrid consists of three generators supplying a demand of 5 MW. Fig. 1 gives the topology of the grid together with the capacity limits of each transmission line and each generator and load. The generator located at bus 4 provides primary reserve, initially with a droop of 12 MW/Hz and later with 4 MW/Hz. The maximum allowed frequency deviation is ± 0.1 Hz. We first assume that all transmission lines have a power transfer capacity of ± 10 MW, which is adequate to avoid grid limitations. In scenario (d) we add an active constraint in the middle line.

In scenario (a) where only the measure of the power injections is available, it is sufficient to set the power produced by the large generator located at bus 4 for achieving feasible grid operation. The remaining injections can be chosen freely. Note that no additional measurement devices are required.

In scenario (b) we reduce the droop of the generator at bus 4 to 4 MW/Hz. This leads to the additional measurement of the power injections at buses 1 and 2. Although the power injections at buses 1 and 2 can be chosen arbitrarily, they must be monitored so that the power produced by the generator located at bus 4 can be set appropriately to balance the system within the given frequency tolerance.

In scenario (c) the measurement of the line flows is added to the set of potential measurements. In this case, only the measure of the line flow between buses 2 and 3 is required for controlling the set point of the generator at bus 4. Notice that since the load is fixed, the measurement of the line flow between buses 3 and 4 would be equally informative.

In scenario (d), we constrain the capacity of the transmission line connecting buses 2 and 3 to the interval $[-1, 1]$ MW. This possibly represents an active grid constraint if the generators at buses 1 and 2 produce at maximum power. The resulting optimal control configuration consists of placing controller devices at buses 1 and 4 and a measurement device at bus 2. Equivalently, the set point of the generator located at bus 2 could be controlled and the injection at bus 1 measured. In addition observe that the measurement of the power flow on the middle line or on the right line would be valid as well.

We show through these simple examples that algorithm (15) yields sparse configurations of sensors and controllers for each tested situation. While in this case the control realizations could also be verified manually, the situation may become much more complex in larger grids. In Table I we present the solver times for the above scenarios and contrast them with an efficient implementation of the hill climbing approach proposed in [7]. Note that in all cases the proposed MILP performed at least more than 2 times faster than the hill climbing optimization procedure.

Scenario	MILP (ms)	Hill climbing (ms)
(a)	77	160
(b)	78	233
(c)	97	277
(d)	101	330

TABLE I: Total solver times for the simple microgrid.

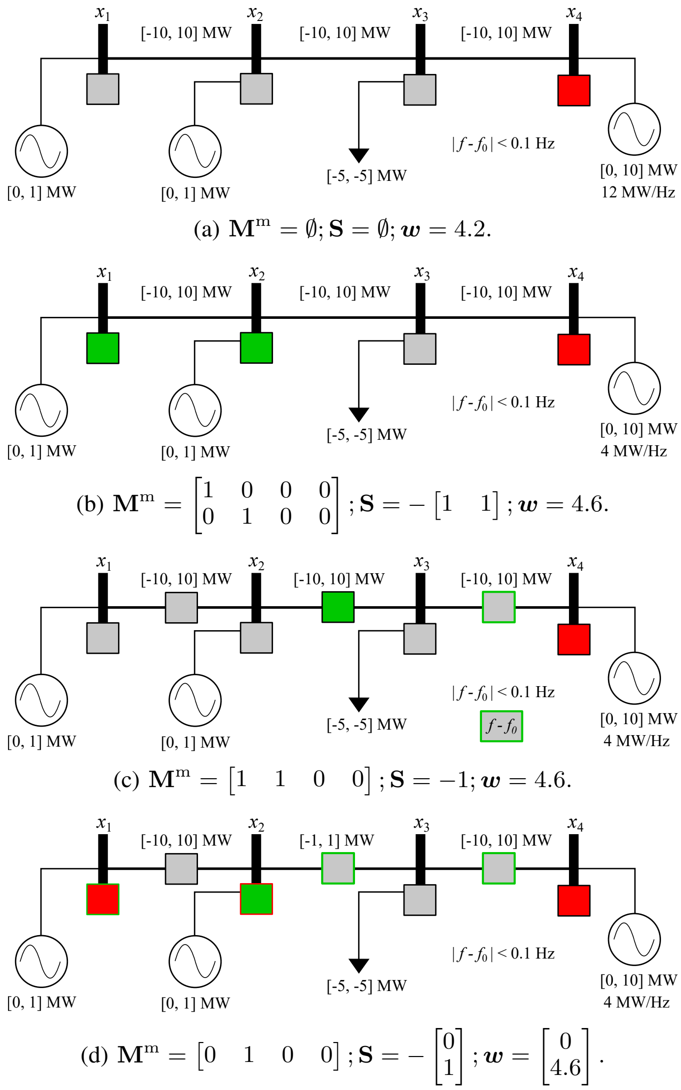

(a) $\mathbf{M}^{\mathrm{m}} = \emptyset; \mathbf{S} = \emptyset; \boldsymbol{w} = 4.2.$

(b) $\mathbf{M}^{\mathrm{m}} = \begin{bmatrix} 1 & 0 & 0 & 0 \\ 0 & 1 & 0 & 0 \end{bmatrix}; \mathbf{S} = -\begin{bmatrix} 1 & 1 \end{bmatrix}; \boldsymbol{w} = 4.6.$

(c) $\mathbf{M}^{\mathrm{m}} = \begin{bmatrix} 1 & 1 & 0 & 0 \end{bmatrix}; \mathbf{S} = -1; \boldsymbol{w} = 4.6.$

(d) $\mathbf{M}^{\mathrm{m}} = \begin{bmatrix} 0 & 1 & 0 & 0 \end{bmatrix}; \mathbf{S} = -\begin{bmatrix} 0 \\ 1 \end{bmatrix}; \boldsymbol{w} = \begin{bmatrix} 0 \\ 4.6 \end{bmatrix}.$

Fig. 1: Minimal sets of controllers and measurements for a simple microgrid of 4 buses connected in line topology. For each test scenario, the measurement set and the realization of the optimal affine-linear control policy are presented. The gray squares represent potential controller/measurement locations. The selected controllers and measurements are highlighted in red and green, respectively. Scenarios (a) and (b) have only the power injections as available measurements, whereas the line flows may also be measured in (c) and (d). For scenarios with multiple, equivalent optimal solutions, the colored frames denoted alternative optimal solutions. The rationale behind the scenarios is as follows: In (b) the primary control droop is reduced compared to (a). In (c) we allow additionally for line measurements. In (d) we reduce the transfer capacity of the middle link to form a potentially active constraint.

B. IEEE 30 Bus Test Case

We now design the control policy for a modified version of the IEEE 30 bus test case, shown Fig. 2. This network consists of 6 generators, 20 loads, and 41 transmission lines. The topology of the power system, the nominal load values, the capacity of the lines and the generators located at buses $\{1, 2\}$ were taken from [9]. We assume that the remaining generators have a capacity of $[0,\ 50]$ MW. We also presuppose that each generator can be scheduled in the range of 10%-90% of its available capacity. In addition, we admit 10% of uncertainty of each load in both directions. The maximum allowed frequency deviation is taken as ± 0.1 Hz. In scenario (a) we only consider the nodal power injections as potential measurements. We obtain a set of 3 controller and 7 measurement devices. In scenario (b) we include the line flows as potential measurements. The solution of MILP (15) reduces the number of required measurements from 7 to 3 while keeping the same controller set obtained in scenario (a). The realization of the affine-linear control policy for scenarios (a) and (b) is not provided due to space limitations.

When performing the MILP optimization for scenario (a), the optimal solution was computed in about 18 s. For scenario (b), however, the optimal solution was computed in 224 s approximately.

VI. Outlook

The algorithm developed in this work extends the approach presented in [7] to design sparse affine-linear control policies for linear power systems. Although we obtained satisfying solver times for the above exemplary power networks, the efficiency of the proposed algorithm has still to be improved in order to address large scale applications.

References

[1] S. Pequito, S. Kar, and A. P. Aguiar, "A framework for structural input/output and control configuration selection in large-scale systems," *IEEE Transactions on Automatic Control*, vol. 61, no. 2, feb 2016.

[2] A. Vaccaro, C. A. Canizares, and D. Villacci, "An affine arithmetic-based methodology for reliable power flow analysis in the presence of data uncertainty," *IEEE Transactions on Power Systems*, vol. 25, no. 2, pp. 624–632, may 2010.

[3] A. Vaccaro, C. A. Canizares, and K. Bhattacharya, "A range arithmetic-based optimization model for power flow analysis under interval uncertainty," *IEEE Transactions on Power Systems*, vol. 28, no. 2, pp. 1179–1186, may 2013.

[4] C. Zhang, H. Chen, H. Ngan, P. Yang, and D. Hua, "A mixed interval power flow analysis under rectangular and polar coordinate system," *IEEE Transactions on Power Systems*, pp. 1–1, 2016.

[5] Y. Wang, Z. Wu, X. Dou, M. Hu, and Y. Xu, "Interval power flow analysis via multi-stage affine arithmetic for unbalanced distribution network," *Electric Power Systems Research*, vol. 142, pp. 1–8, jan 2017.

[6] A. Mešanović, U. Münz, and C. Ebenbauer, "Robust optimal power flow for mixed ac/dc transmission systems with volatile renewables," *IEEE Transactions on Power Systems*, vol. 33, no. 5, pp. 5171–5182, Sep. 2018.

[7] E. Mora and F. Steinke, "On the minimal set of controllers and sensors for linear power flow," *21st Power Systems Computation Conference (accepted)*, 2020.

[8] P. Kundur, N. Balu, and M. Lauby, *Power system stability and control*, ser. EPRI power system engineering series. McGraw-Hill Education, 1994.

[9] A. R. Al-Roomi, "Power flow test systems repository," Halifax, Nova Scotia, Canada, 2015. [Online]. Available: https://al-roomi.org/power-flow

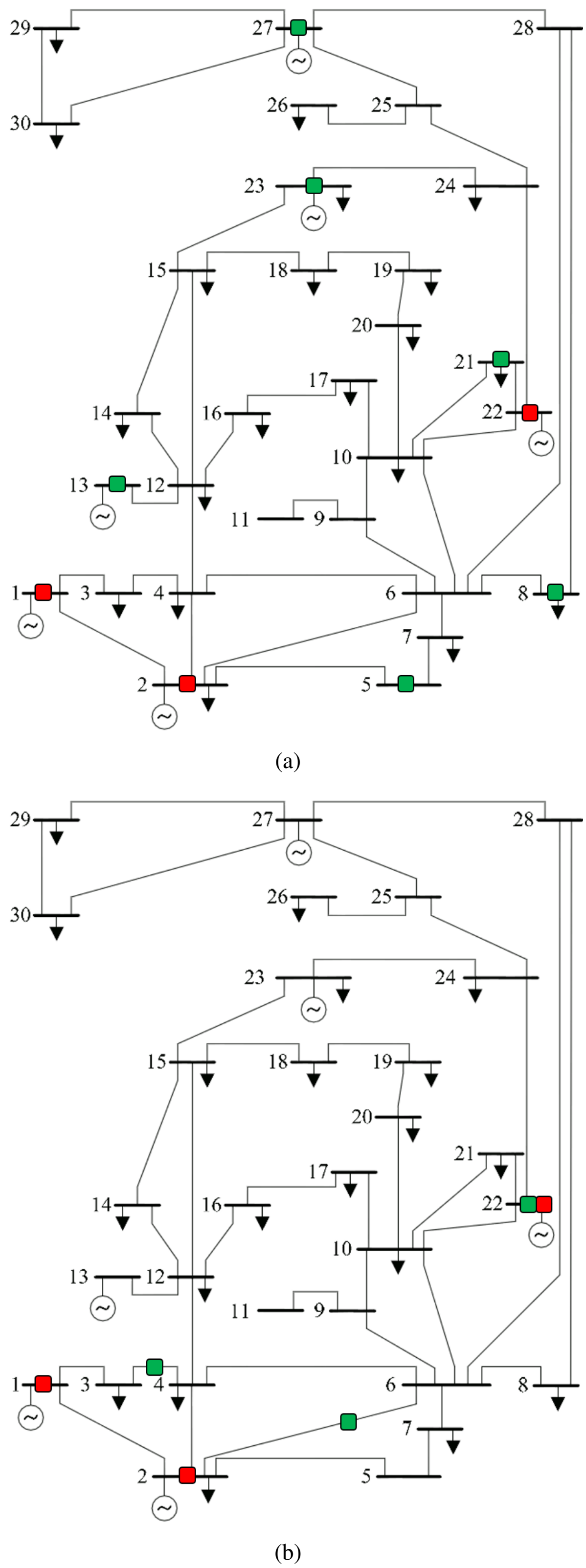

Fig. 2: Minimum sets $\mathcal{C}$ and $\mathcal{M}$ for the modified IEEE 30 bus power system. The location of the selected controllers and sensors is marked in red and green, respectively. In (a) only the injection power injections can be measured. (b) A sparser solution is obtained if the line flows are included into the set of potential measurements.